




AKADÉMIAI KIADÓ

Necking limit analysis of thin wall aerosol can

Jemal Ebrahim Dessie*  and Zsolt Lukacs

Institute of Materials Science and Technology, Faculty of Mechanical Engineering and Informatics, University of Miskolc, H-3515, Miskolc, Egyetemváros, Hungary

Received: December 28, 2021 • Revised manuscript received: March 3, 2022 • Accepted: March 7, 2022
Published online: April 25, 2022

Pollack Periodica •
An International Journal
for Engineering and
Information Sciences

17 (2022) 2, 48–53

DOI:
[10.1556/606.2022.00558](https://doi.org/10.1556/606.2022.00558)
© 2022 The Author(s)

ORIGINAL RESEARCH
PAPER



ABSTRACT

Because of thin wall thicknesses and closed bottom ends of the extruded aerosol can, the necking limit analysis needs intensive investigation. The numerical analysis of the necking process of 0.45 mm thickness pure aluminum aerosol can was carried out. The result indicated that the length of the aerosol can wall, which is not fixed by the bottom die and the angle of inclination of necking tools are important factors that affect the development of deformation boundary limits due to plastic instability of local buckling. The fraction of taper angle of tool becomes more series parameter while necking at larger free length and it needs more concentration. Instead, the ratio of necking tool displacement to the total free length to initiate buckling was increased while increasing free length.

KEYWORDS

aerosol can, local buckling, necking, numerical analysis, pure aluminum

1. INTRODUCTION

The thinner, mostly less than 0.45 mm, the wall thickness of the aerosol can is developed from bulk deformation called impact extrusion. After impact extrusion, narrowing, expansion, and doming are the important forming stages to develop a good appearance and customer-oriented structural shapes. For open-end tubes, hydro-forming is a good approach for the necking process in mass production [1]. Due to the bottom end being closed, very thin wall thickness, and poor formability of the material at room temperature, end press types of forming process are mostly used for the necking process. However, a local buckling failure associated with the necking is the main problem due to the higher ratio of the tube diameter to tube thickness [2]. When designing the necking process, the effect of material damage and strain path on the initiation of local buckling should be properly predicted. Then, studying the effect of necking process parameters can help to model buckling failure in a better way.

M. J. Davidson [3] investigated finite element-based analysis of punch angle, tube temperature, and expansion ratio effect on tube expansion of aluminum alloy. The authors suggested the calculated peak load and energy absorption required for various expansion tool angles to analyze the expansion process of the tube. They have used Taguchi design [3] of experiment and ANalysis Of VAriance, (ANOVA) to optimize results. The effect of loading paths on the expansion ratio limit of warm hydroforming to determine wrinkling behavior was studied by Z. J. Tang [4]. By using both numerical simulation and experimental investigation, the authors point out the effects of axial feeding amount on wrinkling of magnesium alloy tubes [4]. Avalle and Massimiliano [5], investigated experimental and numerical characterization of tube expansion to develop a finite element model. LS-DYNA code was implemented for the finite element analysis to optimize the expansion process parameters of Cu-Ni alloy [5]. Y. Li and Z. You [6, 7] studied the external inversion of thin-walled corrugated tubes using Abaqus explicit code to determine buckling and inversion. The external inversion mode of deformation of aluminum tubes over a constant die profile was analyzed in detail by using a finite element code FORGE2 [6, 7]. Kajikawa and Shohei [8]

*Corresponding author.
E-mail: metjema@uni-miskolc.hu

studied the Finite Element Method (FEM) analyses and experimental studies of the tube drawing process to increase the diameter of the tube and reduce the thickness as well. The maximum flaring ratio was determined to indicate the flaring limit before buckling [8]. D. A. Potianikhin and B. N. Maryn [9] investigated a finite element-based analysis of aluminum alloy tubes by rigid die. The authors were used ANSYS code to define the maximum and residual stresses on the workpiece [9]. Numerical simulation of aerosol can design under pressure and buckling loads using ANSYS code was studied by F. Belblidia and T. N. Croft [10]. The authors were used nonlinear numerical analysis to predict the level of pop-up and burst pressure value that causes tube wall buckling. Numerical findings were validated by physical experiments for reliability [10]. T. Wen et al. [11] investigated the die-less incremental tube-forming process of expansion and narrowing of the tube using experimental and numerical simulation [11]. K. Ahn, J. S. Kim and H. Huh [12] studied the relationship between local buckling and energy absorption for the expansion of thin-wall tubes. A modification of the Plantema equation was considered to predict local buckling supported by numerical analysis [12]. J. E. Bahaoui, L. L. Bakkali, and A. Khamlichi [13] numerically investigated the effect of imperfections on shell buckling strength on thin elastic circular cylindrical shells using the Abaqus software package [13]. A. E. Bouhmid, M. Rougui, and O. Mouhat [14] studied the buckling of symmetrically and anti-symmetrically composite plates with a circular hole. The plate deformation theory and the variational energy method, supported by the finite element method, were applied to find critical loads [14]. S. Nemer and F. Papp [15] investigated the influence of imperfections on the ultimate load due to the buckling resistance of steel beam-columns. Buckling capacities of steel beam-column members were calculated by using four-node shell elements and a non-linear finite element model using Abaqus software [15]. B. P. P. Almeida et al. [16, 17] investigated the expansion and narrowing of 1–2 mm wall thickness Al6060 aluminum alloy tubes using a fixed die. A theoretical and physical experiment supported by numerical simulation was conducted to predict ductile fracture, wrinkling, and necking on the circumference of the tube [16, 17]. However, the authors did not consider the effect of the free length of the workpiece on local buckling, instead, the study considered the ratio of punch diameter with tube diameter because of the open bottom end of the tube.

In this study, due to the small thickness of the aerosol can and the bottom end is closed, only the external surfaces have a chance to be fixed by the bottom die. The effect of aerosol can free length, the length, which is not fixed by bottom die and necking tool angle on the local buckling are numerically determined. Therefore, the safest deformation boundary limit for a single-stage necking operation has been developed and any wall geometries of aerosol can for the specified process parameters should be deformed under the defined safest zone.

2. THEORETICAL ANALYSIS

2.1. Theory of necking process of aerosol can

Necking processes of aerosol can comprise bending, stretching, and compression plastic deformation mechanisms along the circumferential direction. Because of a buckling failure on the wall of the aerosol can, the necking process is currently a challenging issue. In this study, the necking limit was numerically analyzed to accomplish defect-free narrowing and expansion process to develop 12 bar E50KHA1-1_L aerosol can by Mátramétal Ltd standardization [18]. The work plan of the necking process in this company was set up consecutively by considering forming differences (the difference between D_o and D_f) as the main parameter that predict the force balance between each stage. The consecutive geometrical setup of the necking process is shown in Fig. 1. Many other factors that affect the necking of thin-walled aerosol cans are the free length of the workpiece, general necking tool angle, forming velocity, friction factor, etc.

2.2. Local buckling of thin wall tube

Equations (1)–(3) indicated the most common model of the Plantema equation for predicting the inelastic local buckling of a pipe [19],

$$\sigma_{cr} = \sigma_y, \text{ for } \alpha \geq 8, \quad (1)$$

$$\sigma_{cr} = (0.75 + 0.031\alpha)\sigma_y, \text{ for } 2.5 \leq \alpha \leq 8, \quad (2)$$

$$\sigma_{cr} = 0.33\alpha\sigma_y, \text{ for } \alpha \leq 2.5, \quad (3)$$

where, σ_{cr} is the critical stress for local buckling; σ_y is the yield stress; α is the non-dimensional local buckling parameter, which can be expressed for a circular tube as Eq. (4),

$$\alpha = \left(\frac{E}{\sigma_y}\right) \left(\frac{t}{D}\right), \quad (4)$$

where, t is the tube thickness; D is the tube diameter.

But all the above equations, cannot predict the accurate local buckling load due to contact pressure because the model

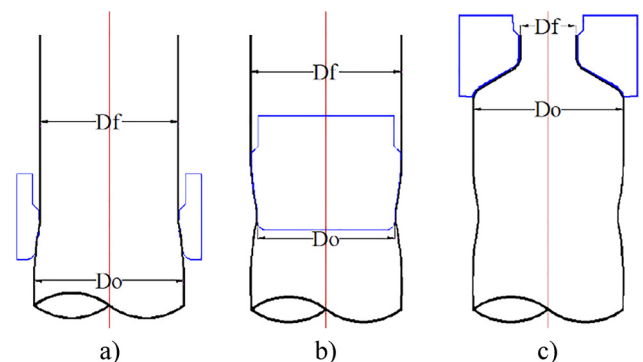


Fig. 1. Geometrical set up: a) narrowing; b) expansion; c) necking

did not include the strain hardening effect. Equation (5) predicts the accurate force due to contact pressure considering the strain hardening effect of material [19],

$$P_{cr} = 2\pi R t (\sigma_y + K \varepsilon_{cr}^n), \quad (5)$$

where P_{cr} is the critical load for buckling; $\sigma = \sigma_y + K \varepsilon_{cr}^n$ is the Ludwik model; ε_{cr} is the buckling strain; K is the material-dependent strength coefficient; R is the tube radius.

The relationship between tube dimension and the critical strain for local buckling can be calculated using Eq. (6),

$$\varepsilon_{cr} = k \left(\frac{t}{R} \right)^2, \quad (6)$$

where k is a material-related fitting parameter.

Therefore, Eq. (3) can be yielded as Eq. (7),

$$P_{cr} = 2\pi R t \left[\sigma_y + K \left\{ k \left(\frac{t}{R} \right)^2 \right\}^n \right]. \quad (7)$$

3. FINITE ELEMENT MODELING

The Finite Element (FE) model in this study was carried out using Abaqus commercial FE software. The isotropic material response was assumed then the FE model developed for this study comprised a two-dimensional axisymmetric element (CAX4), with a finer mesh. The model is composed with the necking tool and the die as a rigid body, and one deformable workpiece. So, only the mechanical properties of the deformable workpiece are important for the finite element model. The contacts between the necking tool and workpiece were treated as lubrication conditions and the Coulomb friction model was used with a constant coefficient of friction of 0.12 [4]. The predicted force due to contact pressure corresponding to vertical displacement of the necking tool is recorded as the FE-predicted load-displacement curve. The elastic properties are defined using Young's modulus, $E = 68,900$ MPa, and Poisson's ratio, $\nu = 0.33$.

3.1. Material model

The effect of strain hardening on buckling is higher in many light metals. In this study, Hollomon strain-hardening equation has been used to develop the true-stress and true-strain curves, which are necessary to describe the tensile flow and strain hardening behavior of the material. Equation (8) described strain-hardening equation:

$$\sigma = K \varepsilon^n, \quad (8)$$

where σ is the flow stress; K is the strength coefficient; ε is the strain; n is the strain-hardening exponent.

The work material was commercially pure aluminum, DIN Al99.5. The flow curve data of the material is summarized in Fig. 2 and the data was referred from the material library of Scientific Forming Technologies Corporation (SFTC) in the DEFORMTM program.

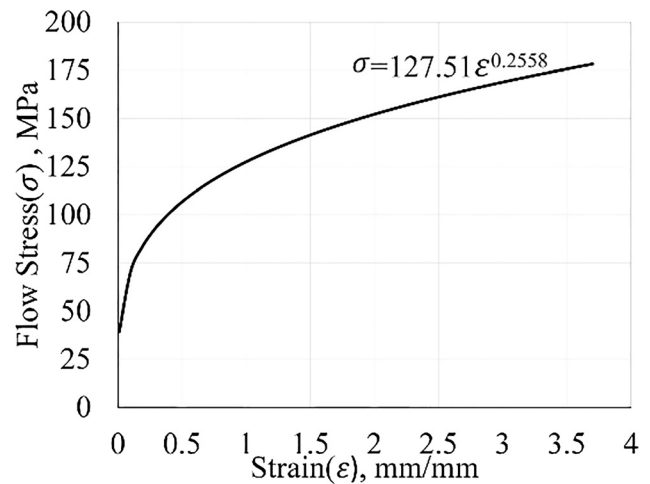


Fig. 2. Flow curve of workpiece material

3.2. Necking limit of aerosol can by buckling

Because of thinner thickness and the closed bottom end of the aerosol can, the necking limit by buckling due to contact pressure needs special investigation. Narrowing and expansion with a rigid necking tool is a convenient approach to analyze buckling of aerosol can due to contact pressure applied between the interface of the workpiece and necking tool. Then, the taper angle of the necking tool (α) and the free length, the length, which is not fixed by the bottom die, (L) of the workpiece are important parameters. The bottom die is completely fixed and there was no relative displacement between the bottom die and workpiece. The necking tool is only free to move vertically and it was set at a velocity of 100 mm s^{-1} . Without external loading, the uniform zero initial stress and strain state was assumed. The simulation setup and designations are shown in Fig. 3 and parameter variations are summarized in Table 1.

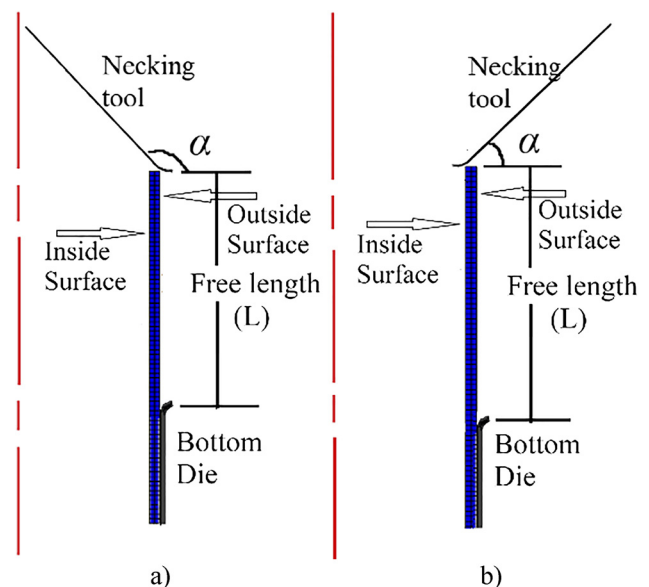


Fig. 3. Simulation setup and notation; a) narrowing; b) expansion

Table 1. Summary of the simulation work plan

Outer diameter, D_o (mm)	Thickness, t_o (mm)	Fillet radius (mm)	Free length, L (mm)	The taper angle of necking tool, α
50	0.45	0.5	10, 20, 30, 40,45	For narrowing: $90^\circ-180^\circ$ For expansion: $0^\circ-90^\circ$

4. SIMULATION RESULTS AND ANALYSIS

In this investigation, the combination of critical technical parameters that affect the determination of necking limit for

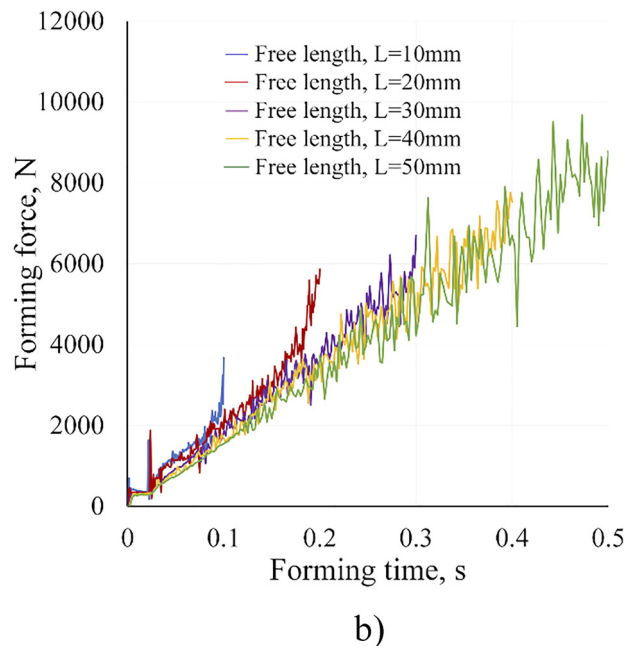
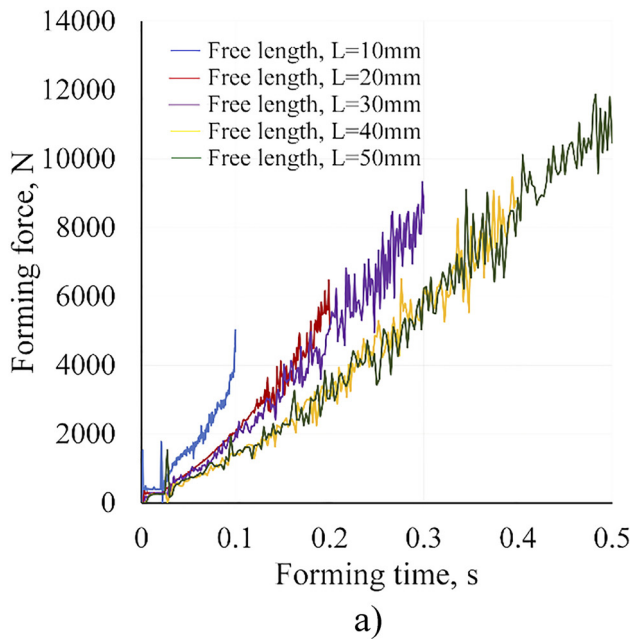


Fig. 4. The total force distribution due to contact pressure: a) narrowing; b) expansion

buckling of the thin wall aerosol has been simulated and examined. Figure 4 summarizes the total force required due to contact pressure at the different free lengths of the workpiece.

The narrowing process requires more load than the expansion process with the same free length of the workpiece as it is indicated in Fig. 5. Of course, once the free length of the workpiece increases, the required deformation

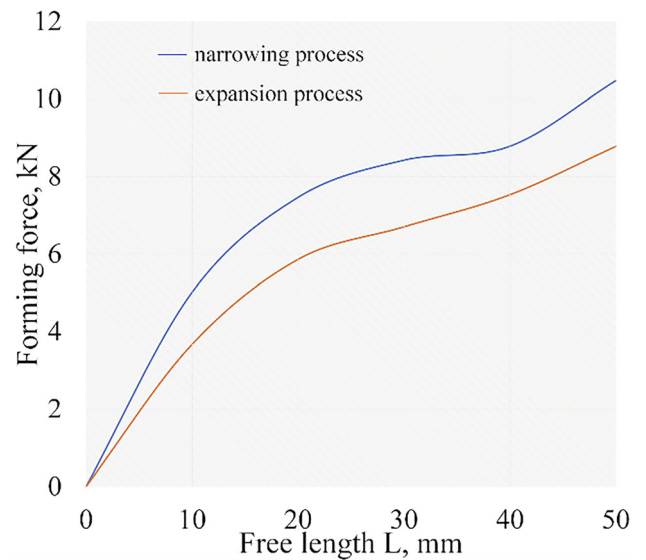


Fig. 5. Effect of the free length of the workpiece for forming load required

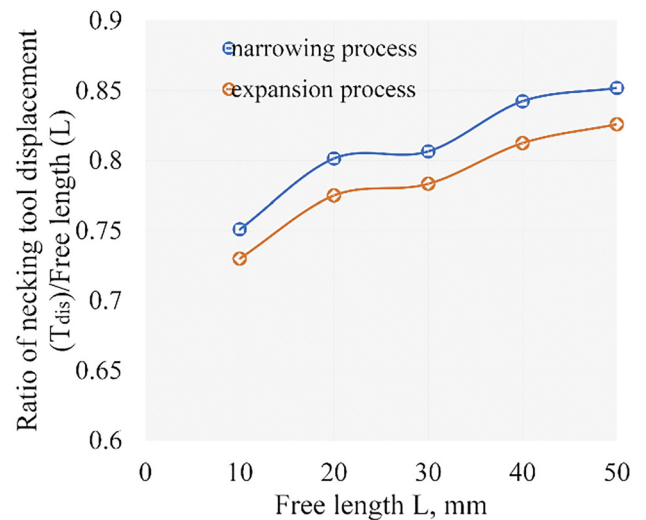
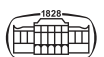


Fig. 6. The effect of the free length of workpiece on the percentage of buckled height workpiece



load increases due to increasing contact length of the necking tool with the workpiece.

The percentage of necking tool displacement (T_{dis}) to initiate local buckling for both narrowing and expansion processes at different free lengths (L) is indicated in Fig. 6. The figure indicated that maximizing free length will increase the percentage of necking tool displacement to initiate local buckling. Simultaneously, the percentage of the buckled walls of aerosol can be high at a small amount of free length (L). Figure 7 shows the effect of the taper angle of the necking tool on the effective plastic strain and the necking tool displacement (T_{dis}) at 30 mm free length (L). The figure also indicated that the fractional degree change of taper angle of the necking tool (α) has initiated local buckling.

The effect of the free length (L) and taper angle of the necking tool (α) on the deformation boundary zone for a single-stage operation is shown in Fig. 8. As the figure

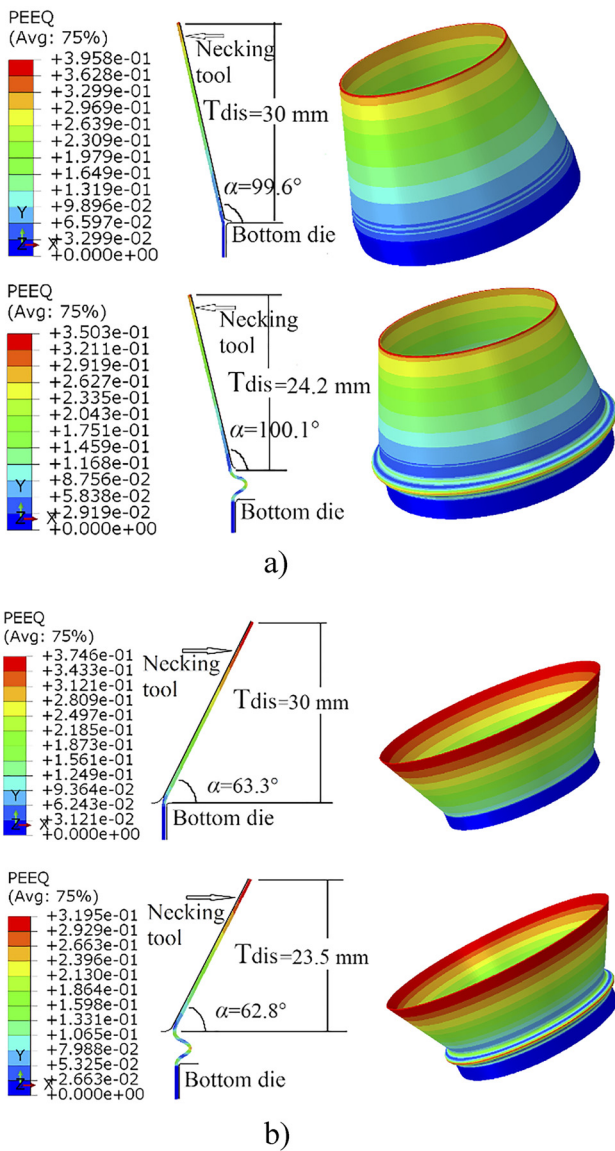


Fig. 7. Effective plastic strain distribution of safe and buckled deformation at 30 mm free length: a) narrowing; b) expansion

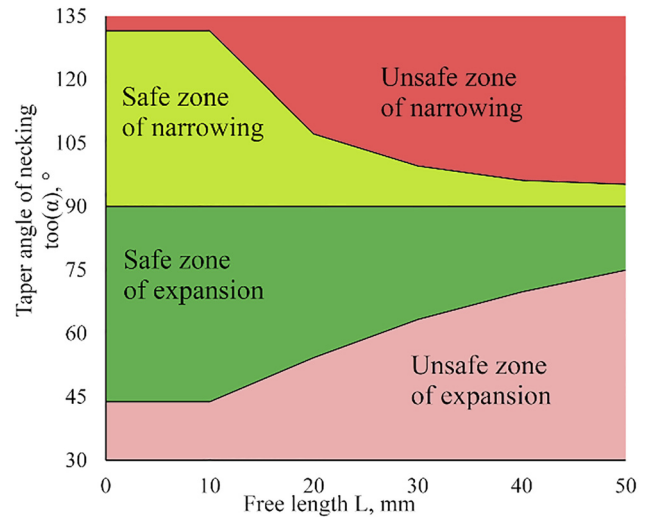


Fig. 8. Boundary limit and deformation zones of narrowing and expansion process

Table 2. Necking limit of aerosol can due to plastic instability of local buckling

Expansion	Taper angle of necking tool (α)	Free length (L) mm
	0–43.83	Unsafe
	43.83–74.99	Safe
	74.99–90	>50
Narrowing	Taper angle of necking tool (α)	Free length (L), mm
	90–95.25	Safe
	95.25–131.51	Unsafe
	131.51–180	any

indicated the safest taper angle of the necking tool for narrowing is between 90 and 131.51° and greater than 131.51° local buckling have initiated. On the other hand, between 43.83° and 90° is the safest necking tool angle for the expansion process and at less than 43.83° buckling and inverting, mostly for small free length, have been initiated. A design monogram of the boundary regions and the choice of the right combination of numerical simulation experiments and technological parameters of end forming of aerosol can for the plastic instability of local buckling summarized in Table 2.

5. CONCLUSION

In the necking operation of the aerosol can, the local buckling load required could not be accurately predicted without considering the diameter of the workpiece, the thickness of the workpiece, plastic strain hardening of the material, necking tool geometry, and work holding mechanism. Specifically, necking tool angle and none fixed wall of aerosol can are important parameters to determine necking boundary regions associated with local buckling. The effect



of free length and the necking tool angle to force balance due to contact pressure was numerically determined. The amount of necking tool angle at different free lengths for both narrowing and expansion processes to initiate local buckling was properly specified. Therefore, the safe and unsafe zone of necking operation was graphically defined. Then, it is easy to choose the number of stages or iterations required to accomplish the required operation without any imperfection. It could also be important to design environment-friendly structural shapes and replace pure aluminum with aluminum alloy to increase the strength and reduce the thickness. By this, it will reduce the volumetric material required and the cost of material for a single aerosol can.

ACKNOWLEDGMENTS

The Authors gratefully acknowledge the project GINOP-2.2.1-15-2017-00035 entitled “Development of the production of aluminum packaging devices (aerosol bottles)”, in which the University of Miskolc, Hungary supported by Mátramétál Ltd.

REFERENCES

- [1] J. P. Magrinho, M. B. Silva, G. Centeno, F. Moedas, C. Vallengano, and P. A. F. Martins, “On the determination of forming limits in thin-walled tubes,” *Int. J. Mech. Sci.*, vol. 155, pp. 381–391, 2019.
- [2] R. D. Ziemian, Ed., *Guide to Stability Design Criteria for Metal Structures*. Wiley- Interscience, Hoboken, 2010.
- [3] M. D. Jakirahemed, M. J. Davidson, G. Venkateswarlu, and L. Venugopal, “A study on effect of process parameters on the expansion of thin-walled aluminum 7075 tubes,” *Int. J. Adv. Sci. Technol.*, vol. 36, pp. 83–94, 2011.
- [4] Z. J. Tang, G. Liu, Z. B. He, and S. J. Yuan, “Wrinkling behavior of magnesium alloy tube in warm hydroforming,” *Trans. Nonferrous Met. Soc. China*, vol. 20, no. 7, pp. 1288–1293, 2010.
- [5] M. Avale, P. C. Priarone, and A. Scattina, “Experimental and numerical characterization of a mechanical expansion process for thin-walled tubes,” *J. Mater. Process. Technol.*, vol. 214, no. 5, pp. 1143–1152, 2014.
- [6] Y. Li and Z. You, “External inversion of thin-walled corrugated tubes,” *Int. J. Mech. Sci.*, vol. 144, pp. 54–66, 2018.
- [7] P. K. Gupta, “Numerical investigation of process parameters on external inversion of thin-walled tubes,” *J. Mater. Eng. Perform.*, vol. 23, no. 8, pp. 2905–2917, 2014.
- [8] S. Kajikawa, H. Kawaguchi, T. Kuboki, I. Akasaka, Y. Terashita, and M. Akiyama, “Tube Drawing process with diameter expansion for effectively reducing thickness,” *Metals*, vol. 10, no. 12, 2020, Paper no. 1642.
- [9] D. A. Potianikhin, B. N. Maryn, S. I. Feoktistov, and S. K. Zayar, “Simulation of thin-walled workpieces ends expanding for pipelines making,” *IOP Conf. Ser. Mater. Sci. Eng.*, vol. 510, 2018, Paper no. 012015.
- [10] F. Belblidia, T. N. Croft, S. J. Hardy, V. Shakespeare, and R. Chambers, “Simulation based aerosol can design under pressure and buckling loads and comparison with experimental trials,” *Mater. Des.*, vol. 52, pp. 214–224, 2013.
- [11] T. Wen, C. Yang, S. Zhang, and L. Liu, “Characterization of deformation behavior of thin-walled tubes during incremental forming: a study with selected examples,” *Int. J. Adv. Manuf. Technol.*, vol. 78, nos 9–12, pp. 1769–1780, 2015.
- [12] K. Ahn, J. S. Kim, and H. Huh, “The effects of local buckling on the crash energy absorption of thin-walled expansion tubes,” in *7th International Conference and Workshop on Numerical Simulation of 3D Sheet Metal Forming Processes*, Interlaken, Switzerland, Sep. 1–5, 2008, pp. 799–804.
- [13] J. El Bahaoui, L. El Bakkali, and A. Khamlichi, “Buckling strength of axially compressed thin axisymmetric shells as affected by localized initial geometric imperfections,” *Int. Rev. Appl. Sci. Eng.*, vol. 3, no. 1, pp. 1–14, 2012.
- [14] A. El Bouhmidi, M. Rougui, and O. Mouhat, “Buckling analysis of rectangular plates with centered cut-out subjected to in-plane two directions under different boundary conditions,” *Pollack Period.*, vol. 14, no. 2, pp. 169–180, 2019.
- [15] S. Nemer and F. Papp, “Influence of imperfections in the buckling resistance of steel beam-columns under fire,” *Pollack Period.*, vol. 16, no. 2, pp. 1–6, 2021.
- [16] B. P. P. Almeida, M. L. Alves, P. A. R. Rosa, A. G. Brito, and P. A. F. Martins, “Expansion and reduction of thin-walled tubes using a die: experimental and theoretical investigation,” *Int. J. Mach. Tools Manuf.*, vol. 46, no. 12–13, pp. 1643–1652, 2006.
- [17] M. L. Alves, B. P. P. Almeida, P. A. R. Rosa, and P. A. F. Martins, “End forming of thin-walled tubes,” *J. Mater. Process. Technol.*, vol. 177, no. 1–3, pp. 183–187, 2006.
- [18] Mátramétál Packaging Manufacturer and Sales Limited Liability Company, 2021. [Online]. Available: <https://matrametal.hu/>. Accessed: Apr. 8, 2021.
- [19] K. Ahn, I. G. Lim, J. J. Yoon, and H. Huh, “A simplified prediction method for the local buckling load of cylindrical tubes” (in Korean), *Int. J. Precision Eng. Manufacturing*, vol. 17, no. 9, pp. 1149–1156, 2016.

